

# Relevance Feedback in Text-to-Image Diffusion: A Training-Free And Model-Agnostic Interactive Framework

Wenxi Wang  
2410915@tongji.edu.cn  
Tongji University  
Shanghai, China

Hongbin Liu  
2253689@tongji.edu.cn  
Tongji University  
Shanghai, China

Mingqian Li  
2252890@tongji.edu.cn  
Tongji University  
Shanghai, China

Junyan Yuan  
Crispyyuan@tongji.edu.cn  
Tongji University  
Shanghai, China

Junqi Zhang\*  
zhangjunqi@tongji.edu.cn  
Tongji University  
Shanghai, China

## Abstract

Text-to-image generation based on diffusion models has achieved remarkable success. However, in real-world scenarios, users often possess a clear visual intent but struggle to express it precisely in language, resulting in ambiguous prompts that generate images misaligned with their preferences. Existing approaches struggle to bridge this gap, as they typically rely on high-load textual dialogues, opaque black-box model inferences, or expensive dataset-driven fine-tuning. They fail to simultaneously achieve low cognitive load, interpretable preference inference, and remain training-free and model-agnostic. To address this, this paper adapts the relevance feedback mechanism from information retrieval to diffusion models, proposing an interactive framework RFD. In RFD, users replace explicit textual dialogue with implicit, multi-select visual feedback to minimize cognitive load. This effortless interaction allows users to simultaneously express complex, multi-dimensional preferences. To translate this preference feedback into precise generative guidance, we construct an expert-curated feature repository and introduce an information-theoretic weighted cumulative preference analysis. This method only needs to calculate the preference from the current-round feedback and incrementally accumulate it into the maintained preference state to infer user's intent. Unlike black-box methods, this white-box mechanism does not need to concatenate the interaction feedback from each round, fundamentally avoiding the model inference degradation caused by lengthy contexts after multi-round interactions. Furthermore, RFD employs a probabilistic sampling mechanism for prompt reconstruction to balance exploitation and exploration, preventing output homogenization. Crucially, RFD operates entirely within the external text space, making it strictly training-free and model-agnostic. This architectural choice provides a universal plug-and-play solution without prohibitive fine-tuning costs. Extensive experiments demonstrate that RFD effectively captures the user's true visual intent, significantly outperforming baseline approaches in preference alignment.

## CCS Concepts

• **Computing methodologies** → **Computer vision**; • **Information systems** → **Users and interactive retrieval**.

## Keywords

text-to-image generation, diffusion models, relevance feedback, intent alignment

## 1 Introduction

Text-to-image generation based on diffusion models has emerged as a transformative technology in generative AI (e.g., Stable Diffusion [20, 24], DALL-E2 [22], and Midjourney). However, in real-world scenarios, users often possess a clear visual intent but struggle to express it precisely in language [6], inherently resulting in ambiguous prompts that generate images misaligned with their preferences. Next, we briefly review existing methods for preference alignment in diffusion models, which are categorized into training-based and inference-based routes, and subsequently present our contributions.

Early training-based methods (e.g., DDPO [3], ImageReward [40], Diffusion-DPO [34], IterComp [45]) attempt to achieve preference alignment by training a reward model on extensive pairwise human annotations to guide the fine-tuning of diffusion models. However, this paradigm lacks user interaction, fundamentally failing when semantically ambiguous prompts obscure the user's true intent. To mitigate this, methods like Twin-Co [35] leverage user dialogue and diffusion model fine-tuning to iteratively clarify visual intent and improve alignment. Yet, heavily relying on multi-round explicit textual dialogue inevitably shifts the cognitive load of resolving ambiguity directly onto the user. This limitation is particularly pronounced for complex concepts like image composition or artistic style, which users struggle to express precisely in language. Furthermore, these approaches lack model-agnostic flexibility, incurring fine-tuning costs whenever the underlying diffusion model is replaced. To achieve model-agnostic flexibility and reduce user cognitive load, PASTA [19] employs reinforcement learning to train a foundation model (FM) agent on a constructed multi-turn preference dataset. It leverages this agent alongside interaction histories derived from implicit user feedback (e.g., clicking on images) to infer preferences, thereby guiding the diffusion model in image generation. However, this method still incurs prohibitive training costs and restricts users to single-choice feedback, failing to capture multi-dimensional preferences. Furthermore, constrained by its training data and the inference degradation over lengthy contexts inherent in FMs, it strictly supports only a fixed 5-turn preference inference.

\*Corresponding author.

**Table 1: COMPARISON OF METHODS BASED ON PREFERENCE ALIGNMENT STRATEGIES**

Method	User Interaction	Implicit Feedback	White-box Inference	Training-Free	Model-Agnostic	Condition: No High-quality Init-image Required
DDPO, ImageReward, Diffusion-DPO, IterComp	×	×	×	×	×	✓
Twin-Co	✓	×	×	×	×	✓
PASTA	✓	✓	×	×	✓	✓
DNO, DAS, DEMON, SIDiffAgent, RAVEL, RAISE	×	×	×	✓	✓	✓
PromptSculptor, DiffChat, Promptimizer	✓	×	×	✓	✓	✓
APPO	✓	✓	×	✓	✓	✓
MultiBO	✓	✓	✓	✓	×	×
<b>RFD (Ours)</b>	✓	✓	✓	✓	✓	✓

Similar to early training-based methods, initial inference-based approaches (e.g., DNO [30], DAS [12], and DEMON [42]) also lack user interaction. These methods employ pre-trained automated evaluators (e.g., aesthetic predictors or HPSv2) to score intermediate images during the iterative denoising process, guiding the generation toward higher scores by directly manipulating the high-dimensional latent space. To achieve deeper semantic understanding and align with complex prompts, recent inference-based methods (e.g., SIDiffAgent [7], RAVEL [33], and RAISE [10]) incorporate FMs and external knowledge bases for autonomous error detection and auto-correction during generation. All of the aforementioned methods share a critical limitation: due to this complete absence of user interaction, they fundamentally fail to achieve preference alignment when faced with semantically ambiguous prompts. To address this, several interactive methods (e.g., PromptSculptor [38], DiffChat[36], Promptimizer [37]) achieve alignment through users’ explicit textual dialogue, but this feedback mechanism imposes a significant cognitive load. Following the trend toward lower cognitive load, APPO [14] leverages FMs to infer preferences from implicit feedback within multi-round interaction histories. However, this FM-driven process remains an uninterpretable black box, making it difficult to diagnose why specific prompts were generated or how preference shifts occur, while suffering from inference degradation over lengthy contexts, leading to degraded accuracy as historical interaction information accumulates across rounds. Alternatively, MultiBO [21] employs Bayesian optimization to achieve mathematical preference inference. Nevertheless, this approach is designed for "last-mile" refinement, as its optimization process relies heavily on high-quality initial reference images, rendering it ineffective in scenarios where the initial prompt is semantically ambiguous. As summarized in Table 1, existing methods fail to simultaneously achieve low cognitive load, interpretable preference inference, and training-free, model-agnostic capability to address the preference alignment challenge caused by semantically ambiguous prompts.

To address this issue, this work aims to make the following novel contributions:

- We adapt the relevance feedback mechanism for diffusion models and propose RFD, a training-free and model-agnostic interactive

framework. By replacing high-load explicit text dialogue with implicit, multi-select visual feedback (i.e., clicking candidate images), this mechanism effectively minimizes user cognitive load while empowering them to intuitively express complex, multi-dimensional preferences.

- To translate preferences inferred from user feedback into clear guidance for the generation process, we build an expert-curated feature standard repository and design an interpretable, white-box preference inference pipeline for multi-dimensional structured feature extraction, preference analysis and selection. This pipeline iteratively clarifies the user’s visual preferences across successive interactions, thereby aligning the final outputs with their true visual intent.
- Experimental validation demonstrates that RFD achieves superior performance over the baseline approach, with ablation studies confirming the necessity of each core component.

## 2 Related Work

### 2.1 Diffusion Models

Diffusion models were first proposed by Sohl-Dickstein et al. [28], which generate data by learning the reverse denoising process. In recent years, diffusion models have demonstrated significant potential in fields such as style transfer, video generation, and image generation. In the realm of style transfer, researchers have primarily focused on balancing fine-grained spatial structure control with computational costs. To reduce computational costs, Latent Diffusion Models were proposed [24], while parallel conditional encoding mechanisms and lightweight adapters were subsequently introduced to achieve fine-grained decoupling and precise control over image spatial structures [17, 44]. In the field of video generation, research efforts have mainly centered on addressing challenges in spatiotemporal consistency and quality, as well as high computational complexity. For instance, spatiotemporal factorized architectures address computational overhead [8], and structure-guided adversarial training strategies improve structural integrity [41]. Furthermore, some methods conducted in-depth explorations into lightweight designs and keyframe guidance with temporal losses,

respectively, significantly enhancing the coherence and high fidelity of video generation [39, 46]. Regarding image generation, current research focuses mainly on two main challenges. The first category focuses on enhancing foundational visual quality and ensuring semantic consistency between the generated images and text prompts. For these issues, methods have evolved from a reliance on extensive, quality-controlled human-annotated data [2, 5, 26] to AI-driven, fully automated pipelines [1, 29]. The second category aims to achieve alignment with user preferences. As detailed in Section 1, despite the various methods proposed in these areas, the field still lacks a strictly training-free, model-agnostic, and low-cognitive-load interactive framework with white-box interpretability to resolve the intent alignment issue under semantically ambiguous prompts.

## 2.2 Relevance Feedback

Relevance Feedback (RF) is a fundamental technique in Information Retrieval, addressing the deviation between the initial query and the latent intent in user retrieval tasks. Rocchio et al. [23] first established the benchmark for this field in text retrieval. Subsequently, to adapt to the characteristics of Content-Based Image Retrieval, studies extended this paradigm to the visual modality, capturing user feedback through linear weighting and probabilistic models [25, 47]. To break through linear constraints and improve efficiency in high-dimensional spaces, researchers introduced Support Vector Machines and nonlinear classification boundaries, successfully modeling users’ nonlinear preferences [9, 31, 32]. Based on this, to address the challenge posed by high-dimensional indexing, Zhang [43] utilized high-dimensional indexing techniques to accelerate the efficiency of feedback retrieval. Furthermore, to enhance global exploration capabilities and improve global convergence efficiency in complex feature spaces, works such as [4, 11, 16] adopted swarm intelligence algorithms, including Particle Swarm Optimization and the Firefly Algorithm, enhancing retrieval efficiency. With the development of deep learning and foundation models, RF has begun to evolve towards conversational retrieval and query expansion. Some works utilized reinforcement learning to optimize long-term interaction rewards [48], while others combined Large Language Models to construct semantic collaboration layers [15, 27], significantly improving query expansion capabilities in complex scenarios. Despite the fact that existing relevance feedback is quite mature in retrieval tasks, it remains rarely explored in generative tasks.

## 3 Method

This section presents a Relevance Feedback-Driven (RFD) interactive framework for diffusion-based image generation, as illustrated in Figure 1. Specifically, during initialization, RFD uses a diffusion model to generate diverse candidate images based on the user’s semantically ambiguous prompts; users can regenerate candidates until images with reference value emerge, then users express visual preferences through binary “like/dislike” annotations. RFD extracts multi-dimensional image features using VLMs based on the constructed feature-standard repository grounded in expert knowledge. Then, an information-theoretic weighted cumulative preference analysis is employed to infer user preferences from the feedback.

Finally, preference information is converted into natural language prompts that drive the diffusion model to generate new candidate images for user annotation. Through multiple interaction rounds, RFD progressively refines its understanding of user intent, enabling generated results to converge toward the desired visual outcome.

### 3.1 Multi-Dimensional Feature Extraction

In RFD, after users express visual preferences through binary “like/dislike” annotations, the core challenge is transforming such abstract preference information into concrete directions that guide generative models. To address this challenge, we construct a feature-standard repository covering various dimensions of image aesthetics as a bridge between user preferences and generation directions, and leverage VLMs to extract candidate-image features within this feature space to prepare for subsequent preference analysis.

*3.1.1 Feature Standard Repository Construction.* Current methods often rely on FMs to infer user preferences from historical feedback within an open, unbounded semantic space. Although this approach captures general user tendencies to some extent, its lack of explicit boundaries renders the inference overly broad, making it difficult to pinpoint specific aesthetic details. To this end, we introduce an expert-curated repository as a high-quality domain prior. By anchoring visual attributes in professional aesthetic standards, this prior transforms unbounded preference estimation into a highly targeted inference process, thereby effectively narrowing the exploration space and ensuring that the captured intents are precise and aesthetically professional. Specifically, the feature-standard repository in this work is constructed based on expert knowledge from [13], and is further supplemented and refined in collaboration with three senior photographers.

The feature-standard repository is decomposed into eight dimensions comprising 28 features, and the statistical properties of these features are categorized into three types: discrete features, ordinal features, and free-form features. Table 2 presents the complete feature-standard repository. Specifically, discrete features refer to features whose values have no inherent ordering relationship, e.g., artistic style can take values such as realistic or abstract. Ordinal features possess explicit ordering relationships, e.g., color brightness can be represented on a graduated scale from “dark” to “bright.” Free-form features employ natural-language descriptions to capture visual elements that are difficult to standardize, but remain critical for aesthetic evaluation.

*3.1.2 Structured Feature Extraction.* The above feature-standard repository defines “which features should be extracted”. Next, we guide VLMs to perform multi-dimensional structured feature extraction through a hierarchically constrained prompt structure.

The prompt design comprises three components. First, role constraints set the model as an “expert image analyst”, which makes the AI analyze images professionally rather than casually. Second, repository constraints require the model to output based on pre-defined dimensions from the feature-standard repository, keeping results structured. Third, output format constraints enforce strict JSON-only output, making results directly usable for analysis.

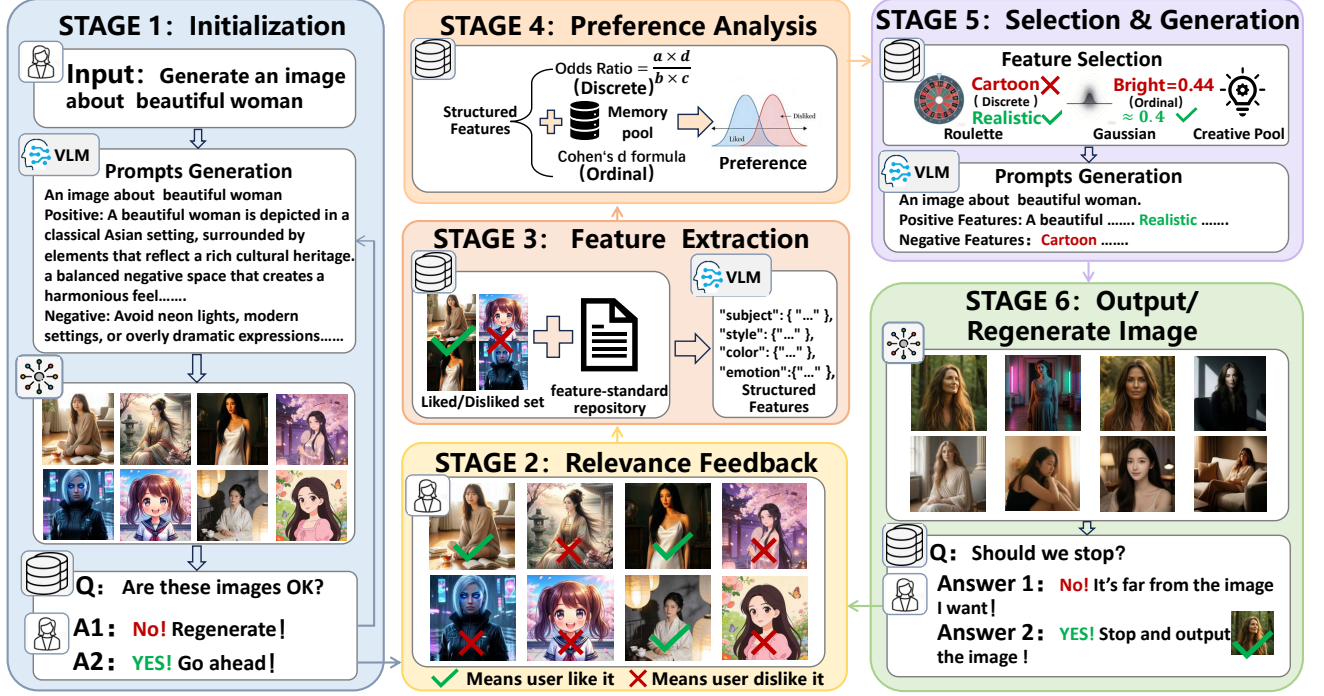


Figure 1: The overall framework of the proposed RFD method.

Table 2: Multi-Dimensional Feature Standard Repository

Dimensions	Feature	Feature Type	Values / Levels
Subject	Subject	Free-form	e.g., "young woman with flowers"
	Subject Type	Discrete	person   animal   landscape   object   ...
Style	Artistic Style	Discrete	realistic   illustration   cartoon   ...
	Era Style	Discrete	classical   vintage   modern   futuristic
	Cultural Style	Discrete	Asian   Western   African   ...
Color	Dominant Colors	Free-form	e.g., "soft pink, lavender, cream"
	Color Palette	Discrete	monochrome   analogous   complementary   ...
	Saturation	Ordinal	desaturated → muted → vibrant
	Temperature	Ordinal	cold → cool → warm → hot
	Brightness	Ordinal	dark → dim → bright → high_key
	Contrast	Ordinal	low → medium → high → extreme
Lighting Type		Discrete	natural   studio   dramatic   backlight   ...
	Composition	Ordinal	closeup → medium → wide
Perspective		Discrete	low_angle   high_angle   birds_eye   ...
	Layout	Discrete	centered   rule_of_thirds   symmetrical   ...
Depth	Ordinal	flat → shallow → deep → extreme_deep	
Negative Space	Ordinal	cramped → minimal → balanced → abundant	
Visual Flow	Discrete	static   dynamic   circular	
Background	Background Type	Discrete	solid   gradient   nature   urban   ...
	Environment	Discrete	indoor   outdoor   nature   urban   abstract   ...
	Background Blur	Ordinal	sharp → slightly_blurred → heavily_blurred
Technical	Detail Level	Ordinal	low → medium → high → ultra
	Texture Rendering	Ordinal	flat → subtle → detailed → hyper_realistic
	Edge Treatment	Discrete	hard   soft   mixed   stylized
	Finish Quality	Ordinal	rough → basic → polished → perfect
First Impression	Raw Description	Free-form	e.g., "A dreamy, ethereal portrait"
	Keywords	Free-form	e.g., ["dreamy", "ethereal", "soft"]
Distinctive	Unique Elements	Free-form	e.g., "Glowing particles, ethereal glow"

## 3.2 Information-Theoretic Weighted Cumulative Preference Analysis

With structured features extracted as described in Section 3.1, the subsequent task is to analyze user preferences regarding these features. Given the distinct properties of discrete, ordinal, and free-form features, we tailor our analysis strategies accordingly. Specifically, free-form features (e.g., "Unique Elements") lack fixed value ranges, and their natural-language form allows VLMs to leverage them directly, thus without additional data processing. Accordingly, this section focuses on preference analysis for discrete and ordinal features.

**3.2.1 Discrete Features Analysis.** For discrete features, we focus on evaluating user preferences for each specific candidate value  $v$  (e.g., "art style = realistic"). At each interaction round  $t$ , we construct a  $2 \times 2$  matrix to characterize the relationship between the presence of value  $v$  and user feedback, as shown in Table 3.

Table 3:  $2 \times 2$  Matrix for Feature Value ( $v$ ) at Round ( $t$ )

	Value $v$ Present	Value $v$ Absent
Like	$A_t$	$C_t$
Dislike	$B_t$	$D_t$

Here,  $A_t$ ,  $B_t$ ,  $C_t$ , and  $D_t$  denote the sample counts at round  $t$  for "liked and  $v$  is present," "disliked and  $v$  is present," "liked and  $v$  is absent," and "disliked and  $v$  is absent," respectively. Based on this matrix, the Odds Ratio (OR) is employed to quantify the direction

and strength of user preference for value  $v$ :

$$\text{OR}_t(v) = \frac{A_t \cdot D_t}{B_t \cdot C_t} \quad (1)$$

where  $\text{OR}_t(v) > 1$  indicates a positive preference for the feature value  $v$  at round  $t$ , while  $\text{OR}_t(v) < 1$  indicates a negative preference.

The term  $\text{OR}_t(v)$  captures only the immediate association between value  $v$  and user preference within round  $t$ . If preference inference relies solely on the current round, preferences expressed in earlier rounds would be entirely forgotten, causing the RFD’s understanding of the user to remain confined to a single interaction. Consequently, it is necessary to fuse preference information across historical rounds to form a continuous preference memory. Notably, the differential contribution of each round must be considered: if the distribution of value  $v$  in a round is non-discriminative (i.e.,  $v$  appears in all samples or is absent from all samples), that round provides zero information for inferring preferences regarding  $v$ . To address this, we introduce adaptive weights based on information entropy. Let  $e_t(v)$  denote the occurrence rate of feature value  $v$  among the candidate images in round  $t$ ; the weight is defined as:

$$w_t(v) = -e_t(v) \log_2 e_t(v) - (1 - e_t(v)) \log_2 (1 - e_t(v)) \quad (2)$$

This weight  $w_t(v)$  approaches zero as  $e_t(v) \rightarrow 0$  or  $e_t(v) \rightarrow 1$ , and reaches its maximum when  $e_t(v) = 0.5$ , effectively filtering out non-informative rounds. Accordingly, the cumulative odds ratio for value  $v$  is computed by aggregating weighted historical statistics:

$$\text{OR}(v) = \frac{\left( \sum_{t=1}^T w_t(v) \cdot A_t \right) \cdot \left( \sum_{t=1}^T w_t(v) \cdot D_t \right)}{\left( \sum_{t=1}^T w_t(v) \cdot B_t \right) \cdot \left( \sum_{t=1}^T w_t(v) \cdot C_t \right)} \quad (3)$$

consistent with the single-round metric, a cumulative  $\text{OR}(v) > 1$  signifies a positive preference for value  $v$  across the entire interaction history, whereas  $\text{OR}(v) < 1$  implies the opposite.

**3.2.2 Ordinal Features Analysis.** For ordinal features (e.g., brightness), values are typically represented by a finite number of distinct levels. For subsequent computation, these levels are linearly mapped to the range  $[0, 1]$  in ascending order. On this basis, Cohen’s  $d$  effect size is adopted to measure the user’s emphasis on this ordinal feature:

$$d_t(f) = \frac{\mu_{\text{liked},t}(f) - \mu_{\text{disliked},t}(f)}{\sigma_{\text{pooled},t}(f)} \quad (4)$$

where  $\mu_{\text{liked},t}(f)$  and  $\mu_{\text{disliked},t}(f)$  denote the mean values of the liked and disliked samples on feature  $f$  at round  $t$ , respectively, and  $\sigma_{\text{pooled},t}$  is the pooled standard deviation. The magnitude  $|d_t(f)|$  indicates the user’s emphasis on feature  $f$  during round  $t$ .

Similar to discrete features, historical information must be fused to prevent preference loss. The information quality of each round’s data is critical: if samples at a given round exhibit highly concentrated values on feature  $f$  (i.e., variance approaching zero), that round contributes limited information for inferring user preferences. Accordingly, variance-based weights are introduced:

$$w_t(f) = \min \left( \frac{\sigma_{\text{pooled},t}^2(f)}{0.25}, 1 \right) \quad (5)$$

where  $\sigma_t^2(f)$  is the variance of all samples on feature  $f$  at round  $t$ . Since the theoretical maximum variance for a variable bounded in  $[0, 1]$  is 0.25 (i.e., extreme polarization), this value serves as the normalization baseline.

Subsequently, weighted computations are employed to aggregate multi-round information. For group  $g \in \{\text{liked}, \text{disliked}\}$ ,  $\mu_g(f)$  represents the multi-round weighted average value of group  $g$  on feature  $f$ , defined as:

$$\mu_g(f) = \frac{\sum_{t=1}^T \sum_{i \in \mathcal{S}_{g,t}} w_t(f) \cdot v_i^t}{\sum_{t=1}^T \sum_{i \in \mathcal{S}_{g,t}} w_t(f)} \quad (6)$$

where  $T$  is the total number of rounds,  $\mathcal{S}_{g,t}$  is the sample set for group  $g$  at round  $t$ ,  $v_i^t$  is the normalized value of sample  $i$  on feature  $f$ , and  $w_t(f)$  is the round weight defined in Eq. (5). The weighted variance  $\sigma_g^2(f)$  for group  $g$  on feature  $f$  is defined as:

$$\sigma_g^2(f) = \frac{\sum_{t=1}^T \sum_{i \in \mathcal{S}_{g,t}} w_t(f) \cdot (v_i^t - \mu_g(f))^2}{\sum_{t=1}^T \sum_{i \in \mathcal{S}_{g,t}} w_t(f)} \quad (7)$$

Finally, the cumulative effect size is derived from the weighted statistics:

$$d(f) = \frac{\mu_{\text{liked}}(f) - \mu_{\text{disliked}}(f)}{\sigma_{\text{pooled}}(f)} \quad (8)$$

where the weighted pooled standard deviation is given by:

$$\sigma_{\text{pooled}}(f) = \sqrt{\frac{\sigma_{\text{liked}}^2(f) + \sigma_{\text{disliked}}^2(f)}{2}} \quad (9)$$

Crucially, the magnitude  $|d(f)|$  quantifies the user’s emphasis on feature  $f$ , and indicates that the user exhibits a preference for the level corresponding to  $\mu_{\text{liked}}(f)$ .

### 3.3 Preference-Driven Feature Selection and Prompt Generation

Upon completing the cumulative preference analysis, RFD obtains quantified user preferences for discrete and ordinal features. Based on this aggregated information, the subsequent task is to select appropriate feature values to construct natural-language prompts for the next round of image generation. This section details the specific selection strategies and the prompt construction process.

**3.3.1 Roulette Wheel Sampling for Discrete Features.** For each discrete feature, if the value with the highest cumulative odds ratio is deterministically selected to guide image generation, the resulting images would tend toward high homogeneity, failing to adequately explore the user preference space. To address this, a roulette-wheel sampling mechanism is introduced. This mechanism assigns higher selection probabilities to values with higher odds ratios, thereby maintaining overall consistency with user preferences. Simultaneously, values with lower odds ratios retain opportunities for selection, enabling the generated images to exhibit diverse feature

combinations and preventing the results from becoming overly monotonous. Specifically, let a discrete feature  $f$  (e.g., “artistic style”) contain  $K$  candidate values  $\{v_1, v_2, \dots, v_K\}$ , with corresponding cumulative odds ratios  $\{\text{OR}(v_1), \text{OR}(v_2), \dots, \text{OR}(v_K)\}$ . The sampling probability for each value is computed as follows:

$$P(v_k | f) = \frac{\text{OR}(v_k)}{\sum_{j=1}^K \text{OR}(v_j)} \quad (10)$$

where  $P(v_k | f)$  represents the probability of selecting value  $v_k$  for feature  $f$ . Accordingly, a specific value for feature  $f$  is sampled independently based on this probability distribution.

**3.3.2 Gaussian Sampling for Ordinal Features.** Similar to discrete features, ensuring diversity is equally critical for ordinal features (e.g., brightness) to prevent homogeneous results. To this end, a Gaussian sampling strategy is adopted: while preserving the overall preference trend, it maintains a certain degree of exploration efficiency. Specifically, this sampling applies only to features satisfying  $|d(f)| \geq 0.8$ , which reflects high user emphasis [18]. For each ordinal feature satisfying this condition,  $\mu_{\text{liked}}(f)$  serves as the preference center for sampling:

$$\mu_{\text{center}} = \mu_{\text{liked}}(f) \quad (11)$$

A continuous random variable  $x_f$  is sampled for feature  $f$ :

$$x_f \sim \mathcal{N}_{[0,1]}(\mu_{\text{center}}, \sigma_{\text{samp}}^2) \quad (12)$$

where  $\mathcal{N}_{[0,1]}$  denotes a Gaussian distribution truncated to  $[0, 1]$ , ensuring the sampled value satisfies the normalization constraint. The variance  $\sigma_{\text{samp}}^2$  serves as a hyperparameter controlling the exploration intensity, and is empirically set to  $\sigma_{\text{samp}} = 0.03$ , balancing diversity and stability.

Finally, the sampled continuous value  $x_f$  is mapped to the nearest level to determine the final feature value.

Through this sampling and remapping process, ordinal features can exhibit random variation around the user’s preferred value, thereby enhancing the diversity of candidate images without deviating from the overall preference direction.

**3.3.3 Pool Sampling for Free-form Features.** Unlike the features discussed above, free-form features defined in Section 3.1 (e.g., “Unique Elements”) lack fixed value ranges. Consequently, they are difficult to quantify numerically yet remain critical for capturing the user’s visual preferences. To this end, we adopt a Pool Sampling Strategy. Specifically, we construct a Creative Materials Pool by aggregating textual descriptions extracted from the “liked” image subset. This repository consolidates high-quality descriptive prompts, including:

- **Overall Impression:** Capturing the primary atmosphere or vibe conveyed to the viewer.
- **Unique Elements:** Identifying unique design artifacts or specific object details.
- **Dominant Color:** Recording complex color combinations preferred by the user.

During prompt generation, descriptions are sampled from this pool to enrich the detail expressiveness of generated results.

**3.3.4 VLM-Driven Prompt Generation.** For each candidate image to be generated in the subsequent round, RFD samples specific feature values using the strategies described above, and then leverages a VLM to generate the corresponding natural-language prompt. The generation process adheres to the following constraints:

- **Hard Constraints:** The user’s initial prompt serves as the in-violable core semantic basis. The VLM must ensure that the generated results strictly satisfy the user’s fundamental intent without deviation.
- **Soft Constraints:** The specific feature values determined via Roulette Wheel Sampling and Gaussian Sampling serve as explicit guidance. The VLM is instructed to translate these structured feature values into natural language modifiers, prioritizing semantic coherence by incorporating as many compatible feature values as possible, rather than rigidly enforcing all preferences simultaneously.
- **Creative References:** The descriptive materials sampled from the Creative Materials Pool act as sources for detail enrichment. The VLM selectively integrates these descriptions to enhance the visual expressiveness of the prompt.
- **Format Requirements:** The VLM is required to output structured results containing the following fields:
  - `positive_prompt`: Descriptions of the desired visual content.
  - `negative_prompt`: Specifications of visual elements to be excluded.

Finally, the generated prompts are fed into the diffusion model to generate a new batch of candidate images, thereby initiating the next cycle of user interaction.

## 4 Experiments

This section validates the effectiveness of the RFD framework. We first describe the experimental setup, including the evaluation scenarios, metrics, and baseline methods. We then present the experimental results in comparison with the baseline methods and conduct case analyses on specific examples. Finally, we perform ablation studies to verify the contribution of each core component. All experiments are implemented in Python and executed on a machine equipped with an Intel Core i7-12700KF processor and 32.0 GB RAM.

### 4.1 Experimental Setup

To evaluate the alignment of user intent under semantically ambiguous prompts, we construct a benchmark dataset composed of Ambiguous Prompt–Ground Truth (GT) image pairs. In this setting, the GT image represents the user’s specific latent intent, while the ambiguous prompt serves as the initial user input. Our benchmark covers five representative categories: Person, Animal, Architecture, Landscape, and Object. This choice is motivated by two considerations. First, coverage: these five categories capture the most common types of user requests in text-to-image generation. Second, diversity: Person/Animal images emphasize artistic attributes and background characteristics; Architecture focuses on geometric structures and spatial relationships; Landscape involves lighting atmosphere and color layering; and Object emphasizes material textures and fine-grained details. Evaluating these diverse image

types allows us to verify the generalization of the RFD across different visual content categories. To simulate relevance feedback, we treat the GT image as the user’s target. A VLM then compares each generated output against the GT and selects the ones that are closer to the target, thereby simulating the user’s binary “like/dislike” annotations.

For evaluation, we extract features from the GT and evaluate with two metrics: Feature Match Rate ( $FMR_T$ ) measures the alignment between the most preferred values for all features at the final round  $T$  and the GT in the feature space, defined as  $FMR_T = \frac{|\mathcal{P}_T \cap \mathcal{A}_{GT}|}{|\mathcal{A}_{GT}|}$ , where  $\mathcal{P}_T$  denotes the set of most preferred values for all features in the final round  $T$  and  $\mathcal{A}_{GT}$  denotes the set of feature-values extracted from the GT. In our experiments, the total number of interaction rounds is set to  $T = 10$ . Average Rounds to Convergence (ARC) quantifies how quickly RFD forms stable preferences during interaction, defined as  $ARC = \frac{1}{D} \sum_{d=1}^D \tau_d$ , where  $D$  denotes the number of discrete and ordinal features, and  $\tau_d$  denotes the earliest round in which the preferred value of the  $d$ -th feature achieves the top rank among all other values and maintains it thereafter. To validate the effectiveness of RFD, we compare RFD against a baseline denoted as LLM-based Prompt Optimization (LPO). Specifically, LPO employs an LLM to automatically expand the ambiguous input into a detailed prompt, generating images without leveraging any user feedback. For a fair comparison, we ensure that LPO generates the same number of candidate images as RFD. Furthermore, we conduct 5 independent runs for each category and report the averaged results to mitigate random error. We employ the open-source Qwen-Image-2512 as the base diffusion model for image generation and Qwen3-VL-32B as the VLM.

## 4.2 Experiments Result

**4.2.1 Analysis of Results.** Table 4 presents the quantitative comparison results between the RFD framework and the baseline LPO across five distinct visual categories. Overall, RFD demonstrates significant advantages in both  $FMR_T$  and ARC, validating the effectiveness of the relevance feedback mechanism in addressing semantically ambiguous prompts.

**Table 4: Comparison of RFD and LPO across five categories.**

Case	FMR <sub>T</sub> (%)		ARC	
	RFD (Ours)	LPO	RFD (Ours)	LPO
Person	89.17	55.00	5.40	~
Animal	90.83	56.67	3.83	~
Architecture	84.17	48.33	3.75	~
Landscape	85.83	57.50	4.17	~
Object	91.67	58.33	3.67	~

Note: ~ denotes not applicable (non-iterative).

First, in terms of  $FMR_T$ , RFD exhibits a significant performance advantage across all tested categories. Experimental data show that  $FMR_T$  of the RFD reaches the high range of 84.17%–91.67%, while the baseline LPO remains limited to the interval of 48.33%–58.33%. This substantial performance gap is fundamentally attributed to RFD’s capability for progressive multi-dimensional feature values

convergence. During the interactive process, RFD drives feature value alignment through iterative user feedback: once specific features converge to their preferred values, the memory mechanism of RFD retains these aligned features while progressively refining the remaining feature in subsequent rounds. This cumulative refinement process enables the generated images to progressively approximate the complex feature value combinations of the Ground Truth. In contrast, due to the absence of a feedback-driven convergence mechanism, the multi-round generation of LPO is equivalent to a sequence of independent stochastic sampling. Consequently, the magnitude of its  $FMR_T$  depends entirely on random probability aligns with user-preferred feature values. Second, ARC further validates the efficiency of the exploration guided by RFD. The results indicate that the ARC values for RFD range from 3.67 to 5.40 across various scenarios, implying that users typically require only 4 to 6 rounds of interaction for RFD to capture and stabilize the primary visual preferences. Lacking feedback mechanisms, LPO is unable to accumulate preference information through interaction with the user and thus exhibits no convergence behavior.

**4.2.2 Case Study.** The experiments above validate the superiority of RFD in feature value selection and convergence performance quantitatively. To further illustrate that as features converge gradually, the generated images progressively approach the user’s actual intent, this section presents the interactive evolutionary process of RFD through a representative case. In this case, the semantic ambiguous initial prompt “a beautiful woman” is adopted as input, while the user’s actual visual intent encompasses multiple implicit feature values: A realistic portrait of a western woman, a composition with a centered layout and medium frame, natural background, soft bright lighting, warm color tones, etc. Figure 2 depicts the evolutionary process of RFD across ten interactive iterations. Through analysis of the interactive process, we can clearly observe that the inference of user preferences exhibits three distinct stages.

The first stage is the exploration phase, corresponding to Iteration 1 to Iteration 4. Faced with the semantic ambiguous initial prompt, RFD conducts a exploration in the multi-dimensional feature space based on user feedback, thereby gradually establishes preferences for the overall directions desired by the user, such as western, realistic, etc. The second stage is the exploitation phase, corresponding to Iteration 5 to Iteration 7. At this stage, features including nature and realistic have stabilized, and the RFD begins to deeply explore user preferences across dimensions such as composition and color, etc. Specifically, in Iteration 4, the user selects Candidate Image 2 to favor softer, warmer tones (aiming to depart from the dominant dull green hues), while choosing Candidate Image 3 to prioritize a centered, medium-frame composition. By Iteration 7, the lighting is noticeably softer and the overall color tone is substantially warmer, featuring a centered, medium-frame composition. However, the overall brightness of certain candidates remains slightly insufficient, indicating a need for further convergence.

The third stage is the convergence phase, corresponding to Iteration 8 to Iteration 10. In this stage, the vast majority of features have completed convergence, and RFD performs final fine adjustments on the remaining non-converged features. The user selects

Candidate Images 1, 2 and 4 in Iteration 7, providing further preference signals for brightness optimization. Ultimately, in Iteration 10, the generated candidate images are highly style-matched with the target intent.

This case study shows the superiority of the RFD framework. Starting solely from an concise prompt, the framework incrementally reconstructs the user’s complex multi-dimensional visual preferences through iterative preference refinement, and finally generates images that accurately reflect the user’s latent intent.

### 4.3 Ablation Study

To validate the effectiveness of each core component in the RFD framework, we designed three groups of ablation experiments using the following variants for comparative analysis: w/o History, which eliminates the historical information accumulation mechanism and infers preferences solely from current-round feedback; w/o Weight, which removes the weighting strategy and aggregates statistics from all rounds equally; and w/o Exploration, which replaces the probabilistic sampling mechanism with a deterministic greedy strategy (i.e., selecting the value with the highest accumulated advantage ratio for discrete features and the mean value of the liked group for ordinal features). Table 5 summarizes the experimental results.

Regarding historical information accumulation, the w/o History variant shows significantly inferior  $FMR_T$  and poor convergence (ARC) compared to the RFD framework. This is because preference inference without historical information relies entirely on the user’s selection in a single round. Such isolated feedback fails to capture all of the user’s preferred feature values simultaneously, directly leading to a reduction in  $FMR_T$ . Moreover, since the inference is independent in each round, feature preference values are prone to frequent fluctuations across interactions, making stable

convergence difficult. In contrast, the RFD framework accumulates historical data, ensuring that preferences are retained even if a specific feature is not explicitly involved in the current round, thereby achieving the progressive convergence of multiple feature values.

Regarding the weighting strategy, the w/o Weight variant also exhibits performance degradation. The core issue is that when candidate images in a given round lack discriminability for a specific feature (e.g., all candidates share a realistic style, or their brightness levels are highly concentrated), the feedback provides no informative value for inferring preferences for that feature value. Without weighting, the statistical noise introduced by such low-information rounds dilutes the preference signals from high-quality informative rounds. This causes unnecessary fluctuations in the values of already converged features, ultimately affecting convergence. By down-weighting the contributions of these non-informative rounds, the weighting strategy effectively preserves the robustness of preference inference.

Regarding the sampling strategy, the primary risk of the w/o Exploration variant lies in its tendency to become trapped in incorrect preference values, making error correction difficult. If a user selects an image deviating from their intent in early rounds due to error or insufficient information, the greedy strategy locks into this incorrect value. Nevertheless, experimental results show that w/o Exploration still achieves a moderate result. This is primarily attributed to two factors: First, the VLM employs a soft-constraint strategy during prompt generation; it prioritizes semantic coherence by incorporating as many compatible feature values as possible, rather than rigidly enforcing all preferences simultaneously. Second, the generative model exhibits imperfect adherence to textual constraints; it may occasionally fail to strictly execute the specific instructions. These factors introduce implicit sources of diversity

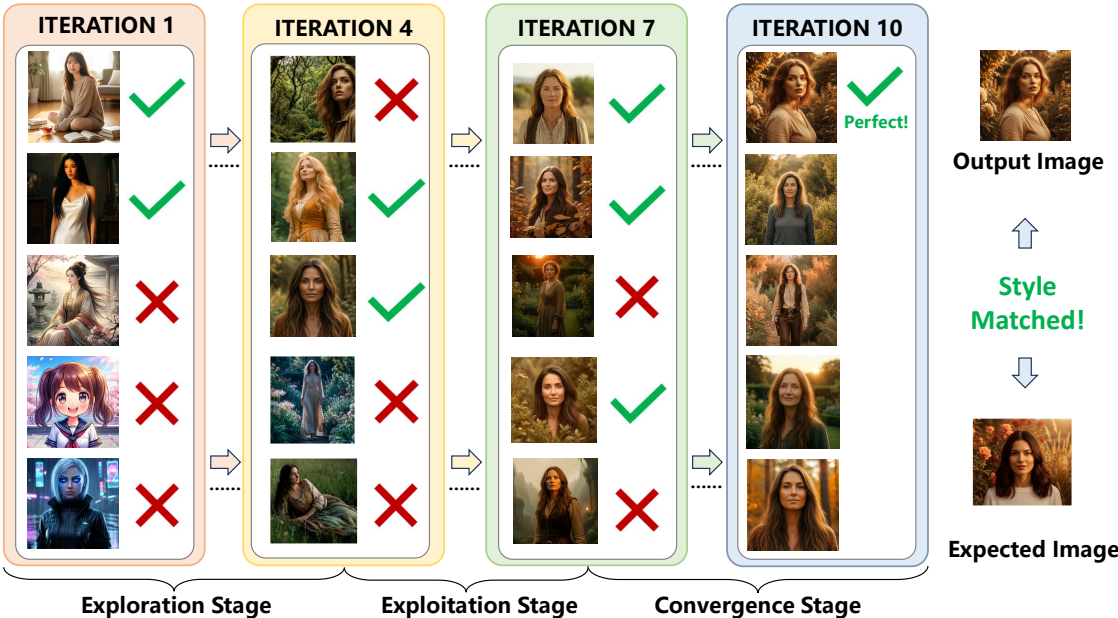


Figure 2: Visualization of the interactive evolutionary process of RFD.

**Table 5: Ablation study results on five categories. We compare RFD with its variants: removing history (w/o History), removing weighting strategy(w/o Weight), and removing the sampling mechanism (w/o Exploration).**

Case	FMR <sub>T</sub> (%)				ARC			
	RFD (Ours)	w/o History	w/o Weight	w/o Exploration	RFD (Ours)	w/o History	w/o Weight	w/o Exploration
Person	89.17	50.00	70.83	62.50	5.40	8.42	6.00	6.08
Animal	90.83	62.50	74.17	71.67	3.83	8.92	5.83	6.04
Architecture	84.17	63.33	75.00	68.33	3.75	7.33	5.16	7.34
Landscape	85.83	57.50	69.17	63.33	4.17	6.41	6.25	4.88
Object	91.67	54.17	77.50	65.00	3.67	6.75	6.75	6.83

into the w/o Exploration variant, partially alleviating the homogeneity of candidate images and providing a chance to escape from incorrect preference values. However, such diversity is uncontrollable as it relies on external randomness. In contrast, RFD maintains the exploration space through probabilistic sampling, providing an explicit correction pathway for recovering from erroneous preferences.

In summary, the ablation experiments confirm that historical accumulation, weighting strategy, and probabilistic sampling are all indispensable components of the RFD framework. The three core components that ensure the continuity, robustness, and exploration efficiency of preference inference, respectively, collectively enable precise intent alignment.

## 5 Conclusion and Future Work

This paper presents RFD, a training-free and model-agnostic interactive framework that addresses the preference alignment challenge caused by semantically ambiguous prompts in text-to-image generation. By adapting the relevance feedback mechanism from information retrieval, RFD enables users to intuitively clarify their visual preferences through implicit, multi-select visual feedback. To translate this feedback into precise generation guidance, we introduce an expert-curated feature repository as a high-quality domain prior, coupled with an interpretable, white-box preference analysis pipeline. This pipeline iteratively clarifies the user’s visual preferences across successive interactions, thereby aligning the final outputs with their true visual intent. Experimental validation demonstrates that RFD achieves superior performance over the baseline approach, with ablation studies confirming the necessity of each core component. While the current feature repository is primarily grounded in general photography principles for everyday image generation, the framework’s plug-and-play architecture possesses immense potential for vertical adaptation. Future work will focus on collaborating with experts in specific fields to construct highly specialized knowledge repositories, thereby extending RFD to solve complex, domain-specific intent alignment problems in professional domains.

## References

- [1] Jingkun An, Yinghao Zhu, Zongjian Li, Enshen Zhou, Haoran Feng, Xijie Huang, Bohua Chen, Yemin Shi, and Chengwei Pan. 2025. Agfsync: Leveraging AI-generated feedback for preference optimization in text-to-image generation. In *Proceedings of the AAAI Conference on Artificial Intelligence*, Vol. 39. 1746–1754.
- [2] James Betker, Gabriel Goh, Li Jing, Tim Brooks, Jianfeng Wang, Linjie Li, Long Ouyang, Juntang Zhuang, Joyce Lee, Yufei Guo, et al. 2023. *Improving image generation with better captions*. Technical Report. OpenAI. <https://cdn.openai.com/papers/dall-e-3.pdf>
- [3] Kevin Black, Michael Janner, Yilun Du, Ilya Kostrikov, and Sergey Levine. 2024. Training Diffusion Models with Reinforcement Learning. In *International Conference on Learning Representations*, B. Kim, Y. Yue, S. Chaudhuri, K. Fragkiadaki, M. Khan, and Y. Sun (Eds.), Vol. 2024. 4965–4987.
- [4] Mattia Broilo and Francesco G. B. De Natale. 2010. A Stochastic Approach to Image Retrieval Using Relevance Feedback and Particle Swarm Optimization. *IEEE Transactions on Multimedia* 12, 4 (2010), 267–277.
- [5] Xiaoliang Dai, Ji Hou, Chih-Yao Ma, Sam Tsai, Jialiang Wang, Rui Wang, Peizhao Zhang, Simon Vandenhende, Xiaofang Wang, Abhimanyu Dubey, Matthew Yu, Abhishek Kadian, Filip Radenovic, Dhruv Mahajan, Kungpeng Li, Yue Zhao, Vladan Petrovic, Mitesh Kumar Singh, Simran Motwani, Yi Wen, Yiwen Song, Roshan Sumbaly, Vignesh Ramanathan, Zijian He, Peter Vajda, and Devi Parikh. 2023. Emu: Enhancing Image Generation Models Using Photogenic Needles in a Haystack. arXiv:2309.15807
- [6] Ritendra Datta, Dhiraj Joshi, Jia Li, and James Z Wang. 2008. Image retrieval: Ideas, influences, and trends of the new age. *ACM Computing Surveys (CSUR)* 40, 2 (2008), 1–60.
- [7] Shivank Garg, Ayush Singh, and Gaurav Kumar Nayak. 2026. SIDiffAgent: Self-Improving Diffusion Agent. arXiv:2602.02051
- [8] Jonathan Ho, Tim Salimans, Alexey A Gritsenko, William Chan, Mohammad Norouzi, and David J Fleet. 2022. Video diffusion models. In *Advances in Neural Information Processing Systems (NeurIPS)*, Vol. 35. 3633–3646.
- [9] P. Hong, Q. Tian, and T. S. Huang. 2000. Incorporate support vector machines to content-based image retrieval with relevant feedback. In *Proceedings of the IEEE International Conference on Image Processing (ICIP)*, Vol. 3. IEEE, 750–753.
- [10] Liyao Jiang, Ruichen Chen, Chao Gao, and Di Niu. 2026. RAISE: Requirement-Adaptive Evolutionary Refinement for Training-Free Text-to-Image Alignment. arXiv:2603.00483
- [11] T. Kanimozhi and K. Latha. 2015. An integrated approach to region based image retrieval using firefly algorithm and support vector machine. *Neurocomputing* 151 (2015), 1099–1111.
- [12] Sunwoo Kim, Minkyu Kim, and Dongmin Park. 2025. Test-time Alignment of Diffusion Models without Reward Over-optimization. In *The Thirteenth International Conference on Learning Representations*. <https://openreview.net/forum?id=vi3DjUHfVm>
- [13] Shu Kong, Xiaohui Shen, Zhe Lin, Radomir Mech, and Charless Fowlkes. 2016. Photo aesthetics ranking network with attributes and content adaptation. In *Proceedings of the European Conference on Computer Vision (ECCV)*, Vol. 9905. Springer, 662–679.
- [14] Zhipeng Li, Yi-Chi Liao, and Christian Holz. 2026. Preference-Guided Prompt Optimization for Text-to-Image Generation. arXiv:2602.13131
- [15] Iain Mackie, Shubham Chatterjee, and Jeffrey Dalton. 2023. Generative relevance feedback with large language models. In *Proceedings of the 46th International ACM SIGIR Conference on Research and Development in Information Retrieval*, 2026–2031.
- [16] A. Mahmood, M. Imran, A. Irtaza, Q. Abbas, and H. Dhahri. 2022. Hybrid evolutionary algorithm based relevance feedback approach for image retrieval. *Computers, Materials & Continua* 70, 1 (2022), 963–979.
- [17] Chong Mou et al. 2024. T2I-Adapter: Learning adapters to dig out more controllable ability for text-to-image diffusion models. In *Proceedings of the AAAI Conference on Artificial Intelligence*. 4296–4304.
- [18] Keith E. Muller. 2012. Statistical power analysis for the behavioral sciences. *Technometrics* (2012).

- [19] Ofir Nabati, Guy Tennenholtz, ChihWei Hsu, Moonkyung Ryu, Deepak Ramachandran, Yinlam Chow, Xiang Li, and Craig Boutilier. 2025. Preference Adaptive and Sequential Text-to-Image Generation. In *Forty-second International Conference on Machine Learning*. <https://openreview.net/forum?id=LCr6CIAEye>
- [20] Dustin Podell, Zion English, Kyle Lacey, Andreas Blattmann, Tim Dockhorn, Jonas Müller, Joe Penna, and Robin Rombach. 2023. SDXL: Improving Latent Diffusion Models for High-Resolution Image Synthesis. arXiv:2307.01952
- [21] Rajalaxmi Rajagopalan, Debottam Dutta, Yu-Lin Wei, and Romit Roy Choudhury. 2026. Personalized Image Generation via Human-in-the-loop Bayesian Optimization. arXiv:2602.02388
- [22] Aditya Ramesh, Prafulla Dhariwal, Alex Nichol, Casey Chu, and Mark Chen. 2022. Hierarchical Text-Conditional Image Generation with CLIP Latents. arXiv:2204.06125
- [23] Joseph J Rocchio. 1971. Relevance feedback in information retrieval. In *The SMART Retrieval System: Experiments in Automatic Document Processing*, G. Salton (Ed.), Prentice-Hall, 313–323.
- [24] Robin Rombach, Andreas Blattmann, Dominik Lorenz, Patrick Esser, and Björn Ommer. 2022. High-resolution image synthesis with latent diffusion models. In *Proceedings of the IEEE/CVF Conference on Computer Vision and Pattern Recognition (CVPR)*, 10684–10695.
- [25] Yong Rui, Thomas S Huang, Sharad Mehrotra, and Michael Ortega. 1998. Relevance feedback: A power tool for interactive content-based image retrieval. *IEEE Transactions on Circuits and Systems for Video Technology* 8, 5 (1998), 644–655.
- [26] Eyal Segalis, Dani Valevski, Danny Lumen, Yossi Matias, and Yaniv Leviathan. 2023. A Picture is Worth a Thousand Words: Principled Recaptioning Improves Image Generation. arXiv:2310.16656
- [27] U. Sharma, S. Rudinac, O. S. Khan, and B. P. Jónsson. 2025. Can relevance feedback, conversational search and foundation models work together for interactive video search and exploration?. In *Proceedings of the IEEE/CVF Conference on Computer Vision and Pattern Recognition Workshops (CVPRW)*, 3779–3788.
- [28] Jascha Sohl-Dickstein, Eric A Weiss, Niru Maheswaranathan, and Surya Ganguli. 2015. Deep unsupervised learning using nonequilibrium thermodynamics. In *Proceedings of the 32nd International Conference on Machine Learning (ICML)*, Vol. 37, 2256–2265.
- [29] Jiao Sun, Deqing Fu, Yushi Hu, Su Wang, Royi Rassin, Da-Cheng Juan, Dana Alon, Charles Herrmann, Sjoerd Van Steenkiste, Ranjay Krishna, and Cyrus Rashtchian. 2025. DreamSync: Aligning text-to-image generation with image understanding feedback. In *Proceedings of the Conference of the Nations of the Americas Chapter of the Association for Computational Linguistics (NAACL)*, 5920–5945.
- [30] Zhiwei Tang, Jiangweizhi Peng, Jiasheng Tang, Mingyi Hong, Fan Wang, and Tsung-Hui Chang. 2025. Inference-Time Alignment of Diffusion Models with Direct Noise Optimization. In *Forty-second International Conference on Machine Learning*. <https://openreview.net/forum?id=JpbqiD7n9r>
- [31] Dacheng Tao, Xiaou Tang, Xuelong Li, and Xindong Wu. 2006. Asymmetric bagging and random subspace for support vector machines-based relevance feedback in image retrieval. *IEEE Transactions on Pattern Analysis and Machine Intelligence (TPAMI)* 28, 7 (2006), 1088–1099.
- [32] Simon Tong and Daphne Koller. 2001. Support vector machine active learning with applications to text classification. *Journal of Machine Learning Research* 2, Nov (2001), 45–66.
- [33] Kavana Venkatesh, Yusuf Dalva, Ismini Lourentzou, and Pinar Yanardag. 2025. RAVEL: Rare Concept Generation and Editing via Graph-driven Relational Guidance. arXiv:2412.09614
- [34] Bram Wallace, Meihua Dang, Rafael Rafailov, Linqi Zhou, Aaron Lou, Senthil Purushwalkam, Stefano Ermon, Caiming Xiong, Shafiq Joty, and Nikhil Naik. 2024. Diffusion Model Alignment Using Direct Preference Optimization. In *Proceedings of the IEEE/CVF Conference on Computer Vision and Pattern Recognition (CVPR)*, 8228–8238.
- [35] Jianhui Wang, Yangfan He, Yan Zhong, Xinyuan Song, Jiayi Su, Yuheng Feng, Ruoyu Wang, Hongyang He, Wenyu Zhu, Xinhang Yuan, Miao Zhang, Keqin Li, Jiaqi Chen, Tianyu Shi, and Xueqian Wang. 2026. Twin Co-Adaptive Dialogue for Progressive Image Generation. arXiv:2504.14868
- [36] Jiapeng Wang, Chengyu Wang, Tingfeng Cao, Jun Huang, and Lianwen Jin. 2024. DiffChat: Learning to Chat with Text-to-Image Synthesis Models for Interactive Image Creation. In *Findings of the Association for Computational Linguistics: ACL 2024*, Lun-Wei Ku, Andre Martins, and Vivek Srikumar (Eds.), Association for Computational Linguistics, Bangkok, Thailand, 8826–8840.
- [37] Leijie Wang, Kathryn Yurechko, and Amy X. Zhang. 2025. Promptimizer: User-Led Prompt Optimization for Personal Content Classification. arXiv:2510.09009
- [38] Dawei Xiang, Wenyan Xu, Kexin Chu, Tianqi Ding, Zixu Shen, Yiming Zeng, Jianchang Su, and Wei Zhang. 2025. PromptSculptor: Multi-Agent Based Text-to-Image Prompt Optimization. In *Proceedings of the 2025 Conference on Empirical Methods in Natural Language Processing: System Demonstrations*, Ivan Habernal, Peter Schulam, and Jörg Tiedemann (Eds.), Suzhou, China, 774–786.
- [39] Zhen Xing et al. 2024. SimDA: Simple diffusion adapter for efficient video generation. In *Proceedings of the IEEE/CVF Conference on Computer Vision and Pattern Recognition (CVPR)*, 7827–7839.
- [40] Jiazheng Xu, Xiao Liu, Yuchen Wu, Yuxuan Tong, Qinkai Li, Ming Ding, Jie Tang, and Yuxiao Dong. 2023. ImageReward: Learning and evaluating human preferences for text-to-image generation. In *Advances in Neural Information Processing Systems (NeurIPS)*, Vol. 36, 15903–15935.
- [41] L. Yang, H. Qian, Z. Zhang, J. Liu, and B. Cui. 2024. Structure-guided adversarial training of diffusion models. In *Proceedings of the IEEE/CVF Conference on Computer Vision and Pattern Recognition (CVPR)*, 7256–7266.
- [42] Po-Hung Yeh, Kuang-Huei Lee, and Jun cheng Chen. 2025. Training-Free Diffusion Model Alignment with Sampling Demons. In *The Thirteenth International Conference on Learning Representations*. <https://openreview.net/forum?id=tfemquulED>
- [43] J. Zhang, X. Zhou, W. Wang, B. Shi, and J. Pei. 2005. Using high dimensional indexes to support relevance feedback based interactive images retrieval. In *Proceedings of the 31st International Conference on Very Large Data Bases (VLDB)*, 1211–1214.
- [44] Lvmin Zhang, Anyi Rao, and Maneesh Agrawala. 2023. Adding conditional control to text-to-image diffusion models. In *Proceedings of the IEEE/CVF International Conference on Computer Vision (ICCV)*, 3836–3847.
- [45] Xinchun Zhang, Ling Yang, Guohao Li, YaQi Cai, xie jiake, Yong Tang, Yujie Yang, Mengdi Wang, and Bin CUI. 2025. IterComp: Iterative Composition-Aware Feedback Learning from Model Gallery for Text-to-Image Generation. In *The Thirteenth International Conference on Learning Representations*. <https://openreview.net/forum?id=4w99NAikOE>
- [46] Daquan Zhou, Weimin Wang, Hanshu Yan, Weiwei Lv, Yizhe Zhu, and Jiashi Feng. 2023. MagicVideo: Efficient Video Generation With Latent Diffusion Models. (2023). arXiv:2211.11018
- [47] Xiang Sean Zhou and Thomas S Huang. 2003. Relevance feedback in image retrieval: A comprehensive review. *Multimedia Systems* 8, 6 (2003), 536–544.
- [48] L. Zou, L. Xia, Z. Ding, J. Song, W. Liu, and D. Yin. 2019. Reinforcement learning to optimize long-term user engagement in recommender systems. In *Proceedings of the 25th ACM SIGKDD International Conference on Knowledge Discovery & Data Mining (KDD)*, ACM, 2810–2818.